Physics Letters A 374 (2010) 4523–4527

Contents lists available at ScienceDirect

Physics Letters A

www.elsevier.com/locate/pla

Laser singular Theta-pinch

A.Yu. Okulov

General Physics Institute of Russian Academy of Sciences, Vavilova str. 38, 119991 Moscow, Russia

ARTICLE INFO

Article history:
Received 20 August 2010
Accepted 6 September 2010
Available online 9 September 2010
Communicated by V.M. Agranovich

Keywords:
Phase singularities
Speckle patterns
Laguerre–Gaussian beams
Ion-acoustic waves
Laser plasma
Magnetic fields

ABSTRACT

The interaction of the two counter-propagating ultrashort laser pulses with singular wavefronts in the thin slice of the underdense plasma is considered. It is shown that ion-acoustic wave is excited via Brillouin three-wave resonance by corkscrew interference pattern of paraxial singular laser beams. The orbital angular momentum carried by light is transferred to plasma ion-acoustic vortex. The rotation of the density perturbations of electron fluid is the cause of helical current which produces the kilogauss axial quasi-static magnetic field. The exact analytical configurations are presented for an ion-acoustic current field and magnetic induction. The range of experimentally accessible parameters is evaluated.

1. Introduction

The stimulated Brillouin scattering (SBS) in a plasma [1,2] is a subject of the considerable interest in several recent decades [3]. The motivation of these research efforts is that a substantial power could be reflected from an underdense plasma via SBS thus limiting the absorption of laser radiation in an inertial confinement fusion (ICF) targets [4]. The possibilities of the ion-acoustic plasma wave resonant seeding by a controllable interference patterns of crossed laser beams [5] were studied in order to manipulate the SBS and Raman scattering [6]. On the other hand the SBS with random phase plates (RPP) is considered as a possible tool for laser beam smoothing and quenching of spatial instabilities in laser plasma [7–9]. The chaotic intensity and phase variations in a speckle pattern induced by RPP are also in use in wavefront reversal SBS mirrors in order to improve phase-conjugated (PC) replica fidelity [10,11]. As is shown recently the dark lines of a speckle (optical vortices) which are collocated with the optical phase singularities [12] inside SBS mirror volume are surrounded by the corkscrew interference patterns [13,14]. These optical helical patterns rotate synchronously with an acoustic angular frequency Ω_{ia} and their rotation is accompanied by a circular motion of the SBS medium inside PC-mirror [15]. Such a circular motion of the medium carries an orbital angular momentum (OAM) [16] extracted from the exciting radiation [15]. In a similar way the transfer of OAM to an ensemble of 10^4 ultracold cesium atoms [17] via rotating interference pattern produced by a pair of the singular Laquerre–Gaussian (LG) laser beams has been observed in a nondegenerate four-wave mixing PC geometry. Quite recently the other example of an optical corkscrew patterns has been demonstrated with photorefractive Ba:TiO_3 PC-mirror [18].

The goal of this Letter is in analysis of a new mechanism of an ion-acoustic wave (IAW) management by means of seeding the corkscrew interference pattern rotating around the isolated optical phase singularity. The qualitative picture is as follows. The optical helical pattern rotates due to a frequency detuning $\Omega_p - \Omega_s$ between the pump and Stockes LG beams (Fig. 1) which collide inside freely expanding preformed underdense plasma jet (PJ, Fig. 2) created by evaporation of the solid-state target by nanosecond laser pulse. The parameters are expected to be close to experimental conditions summarized in [7]. The equilibrium atomic density $n_{i,e}$ is in the range $(0.2 - 0.07)n_c$ where $n_c = 1.011 \cdot 10^{21}$ cm^{-3} is the critical density for laser wavelength $\lambda = 1.05$ μm [7]. We suppose the detuning is adjusted in resonance with IAW having frequency $\Omega_{ia} \approx 2\pi \cdot 10^{12}$ and fast damping rate $\gamma_{ia} \approx (0.5 - 0.1)\Omega_{ia}$ [6,7]. In this SBS strong damping limit when duration of laser pulse is about $\tau \approx 10^{-10-11}$ s the helical density perturbations of the electron (δn_e) and ion (δn_i) liquids of the order of $10^{-2} n_{i,e}$ are collocated with the light intensity maxima. The rotation of the scalar density fields $\delta n_{i,e}$ produces a *nonrelativistic* helical plasma flow with angular frequency Ω_{ia}. This helical current in the neutral plasma reminiscent to the geometry of a *Θ-pinch* [1,2] is expected to produce the axial quasi-static magnetic field. The mechanism discussed here is different from the process of the photon's spin deposit from the circularly polarized intense light pulse to underdense plasma rotation via inverse Faraday effect described in [20,21] and already identified experimentally in [22] by measurement

E-mail address: alexey.okulov@gmail.com.

0375-9601/$ – see front matter
doi:10.1016/j.physleta.2010.09.014

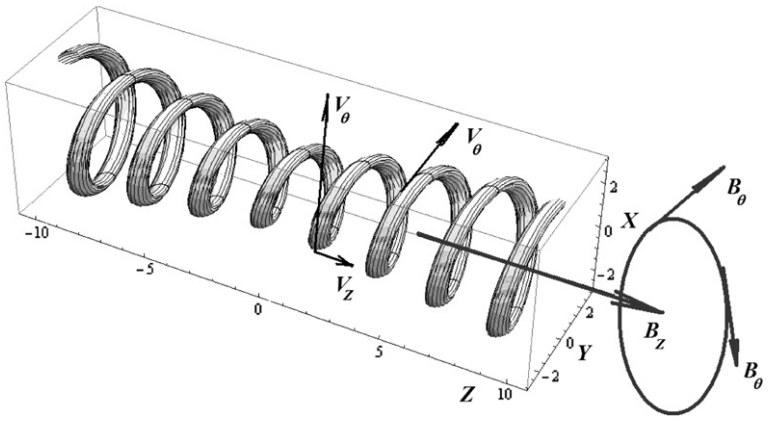

Fig. 1. The isosurfaces of the corkscrew interference pattern [19,13] of a two detuned counter-propagating phase-conjugated LG_0^1 *vortex* laser beams inside plasma jet. (Only one helix of the two is shown.) The rotation of corkscrew pattern causes the motion of a density perturbation δn_e with longitudinal speed $\mathbf{v}_z = \vec{\mathbf{z}} c_{ia}$ and azimuthal speed $\mathbf{v}_\theta = [\Omega_{ia}\vec{\mathbf{z}} \times \vec{R}]$. The solenoidal current produces dipole-like quasi-static magnetic field $\mathbf{B}$. The axial field component $\mathbf{B}_z$ is produced by an azimuthal current density $\mathbf{j}_\theta = 2e\mathbf{v}_\theta \delta n_e$, while the axial current component $\mathbf{j}_z = 2e\mathbf{v}_z \delta n_e$ generates an azimuthal field $\mathbf{B}_\theta$. X, Y, Z scale is in arbitrary units.

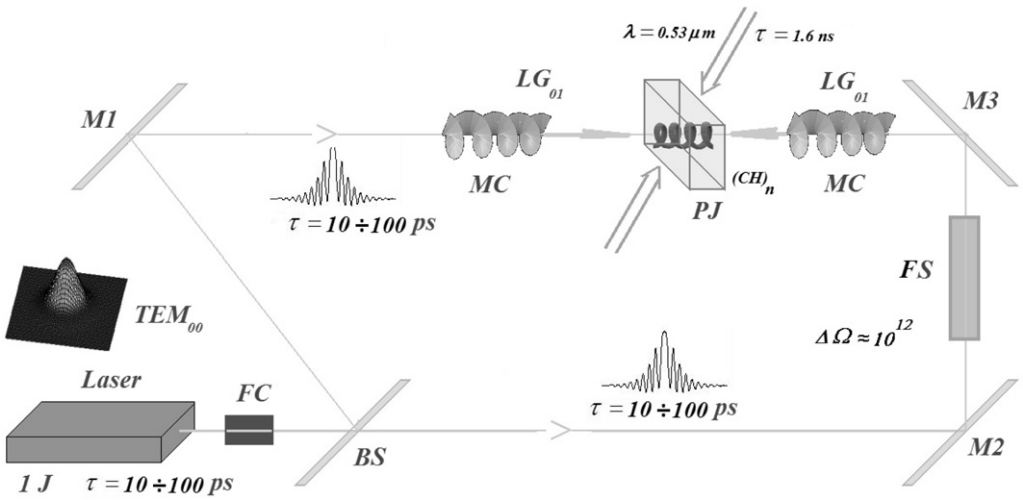

Fig. 2. Conceptual optical loop setup for the colliding pulse SBS excitation in a preformed underdense *plasma jet* **PJ** [7] produced by evaporation of carbon containing plastic film. The beam splitter **BS** divides TEM_{00} Gaussian laser beam into the two pulses. After the passage through the *frequency shifter* **FS** and *mode converters* **MC** [31] the colliding pulses LG_0^1 with a singular wavefronts produce the rotating corkscrew pattern in an expanding **PJ**. Under the proper matching of the rotation frequency $\Omega_p - \Omega_s$ and ion-acoustic frequency Ω_{ia} and under proper management of the path difference and wavefront alignment the rotating helical ion-acoustic wave is expected to be excited. **M1**, **M2**, **M3** are the mirrors, **FC** is a Faraday isolator.

the megagauss (MG) *axial* magnetic induction $\mathbf{B}_z$. In our case the *linearly polarized*, i.e., *zero spin* LG photons [23] transfer their OAM to an ion-acoustic liquid via three-wave Brillouin resonance. The other difference is in the much lower (kilogauss range) magnitude of axial magnetic induction $\mathbf{B}_z$ resulting in the absence of the so-called IAW curtailment [20]. The resulting helical flow of electron liquid (Fig. 1) generates both *axial* and *azimuthal* magnetic inductions $\mathbf{B}_z$ and $\mathbf{B}_\theta$. We will show that interference pattern (Fig. 1) rotates as a "solid body" and the vector of axial speed $\mathbf{v}_z$ (helix *pitch*) is $\lambda/4\pi R$ times shorter than the vector of azimuthal rotation speed $\mathbf{v}_\theta$. Thus the same ratio holds for the current density vectors $\mathbf{j}_z$ and $\mathbf{j}_\theta$. This leads to the corresponding increase of the axial component of magnetic field $\mathbf{B}_z$ compared to azimuthal one $\mathbf{B}_\theta$.

The most interesting issue is the interaction of electron and ion liquids in the process of SBS excitation by a short laser pulse having picosecond duration ($\tau \approx 10^{-10-11}$ s). The standard assumption of the plasma quasi-neutrality on the scales larger than Debye length ($r_D = \sqrt{k_B T_e \epsilon_0 / e^2 n_e} \sim 10^{-6-7}$ cm) requires the instantaneous compensation of the each electron density perturbation by an appropriate motion of the ion liquid. Thus within a framework of the conventional IAW model the macroscopic electron current must be exactly compensated by ionic current and net current ought to be equal to zero resulting in zero magnetic induction. This simple assumption is a basement of the three-wave SBS model (3 scalar "parabolic" PDE) elaborated previously for the subnanosecond plasma flow with keV temperatures [9]. Let us look more carefully to this assumption from the point of view of the optical pulse durations in the range mentioned above (10–500 picoseconds): the experiments followed by analytical estimates [7] and numerical simulations [9] were supposed to have no magnetic fields. But the slight change of duration τ down to the 1 picosecond revealed the substantial magnetic fields [24,25]. Despite the fact of a five order increase of the optical fluxes (up to 10^{19} W/cm^2) the sudden appearance of a MG magnetic field for 1 ps flows requires proper interpretation. The possible interpretation is that a Debye screening does not cancel the net current completely due to partial imbalance in between the ion (n_i) and electron (n_e) liquids. As a result IAW is transformed into magnetosonic wave [1,20]. In order to simplify consideration we will use the steady-state vortex solutions of SBS IAW with phenomenological parameter $\eta \sim 0.01$–0.1 which is the ratio of imbalanced electron current compared to ionic current. The advantage of this simple assumption is in possibility of getting the exact field of velocities and density profile without solving kinetic equation.

It is worth noting the other mechanisms of magnetic fields generation. For example the *axial* currents co-directed with picosecond laser pulse were identified experimentally by Faraday rotation polarimetry as a source of the toroidal magnetic field of the MG range [24,25]. Laser *Z-pinch* formed by return current of the hot electrons ejected from a thin copper wire by an ultrashort laser pulse was studied in [26]. The Weibel instability mechanism is responsible for generation of the quasi-static magnetic fields for the anisotropic electron's density in both nonrelativistic helical plasma flows [27] and intense femtosecond laser pulse in an underdense plasma [28]. The singularities in density and magnetic field growing in time as $(t-t_0)^{-1/2}$ were considered earlier in [27]. The gigagauss magnetic induction **B** mechanisms were discussed in [29,30,26].

2. Helical interference patterns of the Laguerre–Gaussian beams and angular momentum density

SBS is a decay of the quasi-monochromatic electromagnetic wave $\mathbf{E}_p$ into the Stockes wave $\mathbf{E}_s$ and the ion-acoustic wave Q via Bragg scattering. The mechanism of this three-wave parametric instability [7] is the electrostrictive excitation of a sound wave by the moving interference pattern of two waves ($\mathbf{E}_p$ and $\mathbf{E}_s$) detuned by the sound frequency $\Omega_{ia} = 2\Omega_p n_r c_{ia}/c$ [1,2,11], where c_{ia} is the velocity of the ion-acoustic wave, n_r is refractive index. The underdense plasma frequency $\omega_p = \sqrt{n_c e^2/\epsilon_0 m_e}$ is assumed to be smaller than laser frequency $\Omega_p \approx \omega_p/\sqrt{0.2}$.

In quantum terms the decay of the each pump photon to a Stockes photon and an ion-acoustic phonon follows to energy conservation condition $\hbar\Omega_p - \hbar\Omega_s = \hbar\Omega_{ia}$ and to momentum conservation $\hbar\vec{k}_p - \hbar\vec{k}_s = \hbar\vec{k}_{ia} \approx 2\vec{k}_p$ as well. The angular momentum conservation [13] also takes place resulting in OAM deposit in rotating electron liquid (rather than photon's spin deposit [20]). In classical picture the detuning between optical waves Ω_{ia} is a Doppler shift arising due to reflection from sound grating moving with the speed c_{ia} in a medium (plasma) with refractive index n_r. For the backward SBS the period of sound grating $p = \lambda_{ia}$ is approximately equal to a half of exciting wavelength $\lambda_{ia} \approx \lambda_p/2$ (Bragg reflection condition). Noteworthy the Bragg and Doppler conditions are valid both near the bright spots and in the vicinities of the dark lines as well. The fundamental difference of the dark (vortex) lines from the bright spots of the speckle stems from the different structure of their optical wavefronts. In a bright spot the wavefront is parabolic while near a vortex line the wavefront is helicoidal [12,13]. In spite of the statistical nature of a speckle the complex amplitudes of the electric fields $\mathbf{E}_{p,s}$ for the counter-propagating waves could be written analytically inside a given bright or dark spot of a speckle. For a homogeneous polarization state the electric field has the following form in a cylindrical coordinate system (z, r, θ, t) nested in a given spot:

$$\begin{aligned}&\mathbf{E}_{(p,s)}(z,r,\theta,t)\\&\quad=\mathbf{E}^o_{p,s} f_{p,s}(z,r) r^{|\ell|}\\&\qquad\times\exp\bigl[i\Omega_{(p,s)}t \mp ik_{(p,s)}z + i\chi_{p,s}(z,r) \pm i\ell\theta\bigr],\end{aligned}\tag{1}$$

where $f_{p,s}(z,r)$ is a smooth amplitude function elongated in z-direction (e.g. Gaussian one), $\chi_{p,s}(z,r)$ is a smooth phase profile (e.g. parabolic one), ℓ is an azimuthal quantum number (topological charge). Define the mean square root transverse scale of a speckle entity as $\langle D\rangle$. Then mean longitudinal length of a variational speckle functions $f_{p,s}(z,r)$ and $\chi_{p,s}(z,r)$ is the Rayleigh range (Fresnel length) $L_R \approx \langle D\rangle^2/\lambda$ [11]. Both $f_{p,s}(z,r)$ and $\chi_{p,s}(z,r)$ are assumed to be parabolic with respect to r near z-axis. For $\ell = 0$ Eq. (1) describes the phase-conjugation of a bright spot, e.g. zeroth-order Gaussian beam. For $\ell \geqslant 1$ and when $f_p(z,r) = f_s(z,r)$ and $\chi_p(z,r) = \chi_s(z,r)$ Eq. (1) describes the perfect phase-conjugation of an optical vortex with ultimate fidelity, i.e., when the correlation integral of the pump $\mathbf{E}_p$ and Stockes $\mathbf{E}_s$ fields is equal to unity [15]. For the ℓ-order LG_0^ℓ beam (LG) the $f_{p,s}(z,r)$ has Gaussian form [13]. Thus two phase-conjugated LG compose in their common waist the corkscrew interference pattern (Fig. 1) [13,15]. Qualitatively the same corkscrew pattern in PC-mirror appears in the vicinity of each optical vortex line of an optical speckle pattern:

$$\begin{aligned}&\bigl|\mathbf{E}_p(z,r,\theta,t) + \mathbf{E}_s(z,r,\theta,t)\bigr|^2\\&\quad=\bigl|\mathbf{E}^o_p\bigr|^2\bigl[1 + R_{pc} + 2\sqrt{R_{pc}}\\&\qquad\times\cos\bigl[(\Omega_p - \Omega_s)t - (k_p + k_s)z + 2\ell\theta\bigr]\bigr] \times r^{2|\ell|} f^2_{p,s}(z,r),\end{aligned}\tag{2}$$

where $R_{pc} = |\mathbf{E}^o_s|^2/|\mathbf{E}^o_p|^2$ is the PC-reflectivity. The maximum of the interference pattern acts as an Archimedian screw transferring OAM from light to the matter [15]. This happens because the orbital part of the electromagnetic angular momentum density M_z of LG is collocated with a maximum of the light intensity [31]:

$$M_z(z,r,\theta,t) \approx \frac{\ell}{\Omega_p}|\mathbf{E}_{p,s}|^2 + \frac{\sigma_z r}{2\Omega_p}\frac{\partial|\mathbf{E}_{p,s}|^2}{\partial r},\tag{3}$$

where $\sigma_z = 0, \pm 1$ corresponds to linear, right and left polarizations of LG respectively. Hence there is a principal difference between a vortex line and a bright spot in the optical speckle. The bright spot only pushes the medium by *rolls* of interference pattern [13] along propagation direction (z-*axis*) of a pump wave $\mathbf{E}_p$, while the vortex line located in a dark spot produces the additional rotational effect upon liquid and imprints the angular momentum therein [15].

3. Optical collider setup for ultrashort laser pulses with a singular wavefronts

The easiest way to produce the optical corkscrew by means of the interference of a pair of the two phase-conjugated optical vortices is to use a *loop* optical setup (Fig. 2) reminiscent to optical collider schemes [32]. Eq. (1) shows that a phase-conjugated optical vortex $\mathbf{E}_s \approx \exp(+ik_s z - i\ell\theta)$ has the same ratio of the signs of the k_s and $\ell\theta$ in a self-similar variable as those of a pump wave $\mathbf{E}_p \approx \exp(-ik_p z + i\ell\theta)$. This means that a helical wavefront of the PC-vortex $\mathbf{E}_s$ has the same value and sign of the topological charge ℓ, as an incident wave $\mathbf{E}_p$. Hence the PC-vortex is absolutely identical to an incident wave except for the exactly opposite direction of propagation. The restriction on the turnover of the direction of propagation is a number of reflections from conventional, i.e., non-PC-mirrors. The *odd* number of reflections changes the topological charge ℓ to the opposite one [13]. Hence the conceptual *loop* setup ought to perform the *even* number of reflections in order to keep the topological charges of colliding pulses identical to each other as shown at Fig. 2. The alternative is to use two mode converters (**MC**) at a final straight path before target **PJ** (also at Fig. 2). The other restriction imposed on *coherence length* means that a path of the counter-propagating vortices ought to be equalized with an accuracy better than $L_{coh} = c\tau$ for proper temporal overlapping.

For the transform-limited light pulses having $\tau \approx 1$–100 ps duration the coherence length is $L_{coh} \approx 3\times10^3$–$3\times10^5$ μm, i.e., above $300\cdot\lambda_p$. In such a case the ultrashort pulses with a singular wavefronts divided by a beamsplitter in a proposed loop scheme (Fig. 2) will collide in a thin slice of a preformed underdense ($\Omega_p > \omega_p = \sqrt{n_e e^2/m_e\epsilon_0}$) plasma jet [7] and produce corkscrew interference pattern therein. Because the SBS sound (IAW) grating parameters must be in a resonance defined by Doppler and Bragg

conditions, the frequency shift between colliding pulses should be equal to the ion-acoustic frequency Ω_{ia} with an accuracy better than ion-acoustic SBS linewidth $\delta\Omega_{ia}$. Such frequency shift could be produced by means of Raman scattering in compressed gases.

The acoustical frequency Ω_{ia} is of the order of 10^9 Hz for SBS in a room-temperature gases and liquids because it is determined by a thermal velocity $V_T \approx \sqrt{k_B T/m_{i,e}}$ at an ambient temperature $T \approx 300$ K (0.025 eV), where k_B is a Boltzmann constant and $m_{i,e}$ is a mass of a particle. The Brillouin linewidth in transparent dielectric is defined by a damping rate of sound [11]. The ion-acoustic plasma frequency shift Ω_{ia} has roughly the same dependence on electron and ion temperatures T_e and T_i. In this case the much higher $T_{i,e} \approx 1$ keV offers the 10^{12} Hz frequency shift due to a basically same square root dependence $c_{ia} \approx \sqrt{k_B T_e/m_i}$, or more precisely $c_{ia} = \sqrt{k_B(Z\cdot T_e + 3T_i)/m_i}$, where Z is the ion's charge [9]. The SBS linewidth for IAW is due to the Landau damping $\gamma_{ia} \sim \nu_L = \Omega_{ia}\sqrt{\pi Z m_e/8m_i}$ [33].

4. Configuration of an ion-acoustic plasma vortex seeded by a corkscrew interference pattern

Below are the SBS equations of motion for the scalar slowly varying envelope optical fields, i.e., $\mathcal{E}_p$ moving in the positive z-direction and $\mathcal{E}_s$ moving oppositely:

$$\frac{\partial\mathcal{E}_p(z,r,\phi,t)}{\partial z} + \frac{n_r}{c}\frac{\partial\mathcal{E}_p}{\partial t} + \frac{i}{2k_p}\nabla_\perp^2\mathcal{E}_p = \frac{i\Omega_p n_e}{4cn_c}\tilde{Q}\,\mathcal{E}_s, \tag{4}$$

$$\frac{\partial\mathcal{E}_s(z,r,\phi,t)}{\partial z} - \frac{n_r}{c}\frac{\partial\mathcal{E}_s}{\partial t} - \frac{i}{2k_p}\nabla_\perp^2\mathcal{E}_s = -\frac{i\Omega_s n_e}{4cn_c}\mathcal{E}_p\,\tilde{Q}^*, \tag{5}$$

and dimensionless slowly varying IAW density perturbation complex amplitude $\tilde{Q}$ [1,2,4,7,9]:

$$\frac{\partial\tilde{Q}(z,r,\phi,t)}{\partial z} + \frac{1}{c_{ia}}\frac{\partial\tilde{Q}}{\partial t} + \frac{2\gamma_{ia}\tilde{Q}}{c_{ia}} + \frac{i}{2(k_p+k_s)}\nabla_\perp^2\tilde{Q} = i(k_p+k_s)\mathcal{E}_p\mathcal{E}_s^*\frac{\epsilon_0}{2n_c k_B T_e}, \tag{6}$$

where $\nabla_\perp = (\partial_x, \partial_y)$, n_c is the critical plasma density [4,9]. For a preformed plasma jet of the thickness $L_{jet} \approx 10^3$ μm [7] probed by two colliding singular laser beams of comparable amplitudes $\mathcal{E}_p \approx \mathcal{E}_s$ (Fig. 2) with beam waist diameter $D \approx 100$ μm and wavelength $\lambda_p \approx 1.05$ μm the Rayleigh range is $L_R = k_p D^2 \approx 10^4$ μm $\approx 10L_{jet}$. Then $\nabla_\perp^2$ terms which are responsible for the transverse effects could be omitted. In the linear regime of SBS and under the weak coupling conditions the fields $\mathcal{E}_p$ and $\mathcal{E}_s$ are close to those fixed at their free-space values at the opposite boundaries of the jet **PJ** and their z-dependence is obtained exactly throughout all inner z. This weak-coupling regime might be justified due to nonsaturated SBS reflectivity ($R_{sbs} \approx 0.03$) obtained in [7]. Next assumption is the stationary SBS regime when IAW damping is assumed to be strong: $\gamma_{ia} \approx (0.5-0.1)\Omega_{ia} > \tau^{-1} \approx 10^{10-11}$ Hz [6,7]. Thus exact expression for the complex amplitude of IAW $Q(z,r,\theta,t) = \tilde{Q}\cdot\exp[i(\Omega_{ia}t - k_{ia}z)]$ follows immediately for the pair of colliding LG vortices [13] with $|\mathcal{E}_p^o| = |\mathcal{E}_s^o|$:

$$Q = \exp\big[i(\Omega_{ia}t - k_{ia}z) + i2\ell\theta\big](r/D)^{2|\ell|} \times \exp\left[-\frac{2r^2}{D^2(1+z^2/(k_p^2D^4))}\right]\frac{\Omega_{ia}}{4\nu_L}\frac{\epsilon_0}{n_c k_B T_e}\big|\mathbf{E}_p^o\big|^2. \tag{7}$$

Consequently the density perturbation field $q(z,r,\theta,t) = \delta n/n_e = Re(Q)$ demonstrates a rotation typical to optical vortex, like LG beam. The difference is in doubled topological charge 2ℓ due to the angular momentum conservation [13,15]:

$$q = \cos[\Omega_{ia}t - k_{ia}z + 2\ell\theta](r/D)^{2|\ell|} \times \exp\left[-\frac{2r^2}{D^2(1+z^2/(k_p^2D^4))}\right]\frac{\Omega_{ia}}{4\nu_L}\frac{\epsilon_0}{n_c k_B T_e}\big|\mathbf{E}_p^o\big|^2. \tag{8}$$

Thus we see that in the colliding pulse geometry the IAW density perturbation q has a form of a double helix which rotates around z-*axis* with the angular frequency Ω_{ia} (Fig. 1). Then an analytical expression for the ion-acoustic current density $\mathbf{j}_{ia}$ could be extracted from the dynamical equations for the electron liquid [1,2]:

$$\frac{\partial q}{\partial t} + \nabla\cdot q\mathbf{V} = 0; \qquad \frac{d\mathbf{V}}{dt} = -\frac{e}{m_e}\big[\mathbf{E} + [\mathbf{V}\times\mathbf{B}]\big]. \tag{9}$$

From the first equation in (9) (continuity equation) the approximate expression for the ion-acoustic current density vector field $\mathbf{j}_{ia}(\vec{r},t)$ may be obtained using following symmetry arguments. The $\dot{q}$ plays the role of the density of effective "charge" density of the long "charged twisted wire", while $q\mathbf{V}$ is an effective "electric field" directed along the normal to this "charged twisted wire" (Fig. 1, $\vec{x}$, $\vec{y}$, $\vec{z}$ are unit vectors). Then the current density is obtained via Gauss theorem:

$$\mathbf{j}_{ia}(\vec{r},t) = 2\eta\ell Z\cdot e\cdot n_e q(\vec{r},t)\mathbf{V} \approx 2\eta\ell Z\cdot e\cdot n_e q(\vec{r},t)\cdot\big[\vec{\mathbf{z}}c_{ia} + \vec{\mathbf{x}}\Omega_{ia}\cdot|\vec{r}|\cos(\Omega_{ia}t) + \vec{\mathbf{y}}\Omega_{ia}\cdot|\vec{r}|\sin(\Omega_{ia}t)\big]. \tag{10}$$

At this point a dimensionless parameter $\eta \sim 0.01$–0.1 was introduced in order to take into account the partial imbalance of electron and ionic currents. When $\eta = 0$ there exist two co-rotating IAW vortices generating the equal currents in a plasma jet and this results in a zero net current. We assume that η is substantially smaller than unity. Thus the net current is smaller than steady state ion current by order of magnitude or more and it has a spatial configuration described by (10). Because the distribution functions $W_{i,e}(\vec{r},\vec{p},t)$ [1] in the proposed geometry (Fig. 1) are expected to be strongly anisotropic and not known yet the usage of dynamical equations (4)–(6), (9) with phenomenological parameter η seems to be reasonable. Then substitution of the *nonrelativistic* $\mathbf{j}_{ia}$ in a Biot–Savarr integral gives the quasi-stationary magnetic field $\mathbf{B}$:

$$\mathbf{B}(\vec{R},t) = \int\frac{\mu_0[\mathbf{j}_{ia}(\vec{r},t)\times(\vec{R}-\vec{r})]}{4\pi|\vec{R}-\vec{r}|^3}d^3\vec{r}. \tag{11}$$

The expression for magnetic induction inside the plasma solenoid (Fig. 1) and near it's end will be published elsewhere. In the far field the time-averaged induction $\tilde{\mathbf{B}}(\vec{R}) = \tau^{-1}\int_0^\tau\mathbf{B}(\vec{R},t)\,dt$ has the configuration of the magnetic dipole, whose sign is determined by the optical topological charge ℓ:

$$\tilde{\mathbf{B}}(\vec{R}) = \frac{\mu_0}{4\pi}\left[\frac{3(\vec{\mu}\cdot\vec{R})\vec{R}}{R^5} - \frac{\vec{\mu}}{R^3}\right]; \quad \vec{\mu} \approx 2\ell\vec{z}\frac{I_{ia}\pi D^2 L_{jet}}{\lambda_p}, \tag{12}$$

where $\vec{\mu}$ is an effective magnetic moment induced by the corkscrew ion-acoustic current $I_{ia} \approx e\cdot\eta\cdot\delta n_{i,e}\cdot\Omega_{ia}\lambda_p D^2/4 \approx 10^{-3}$ A for the optical fluxes $c\cdot\epsilon_0|\mathbf{E}_p^o|^2 \approx 10^{14}$ W/cm^2. The ratio of the axial ($|\tilde{\mathbf{B}}_z| \approx 10^4$ G) to an azimuthal ($|\tilde{\mathbf{B}}_\theta|$) component of a static magnetic field is given by:

$$\frac{|\tilde{\mathbf{B}}_z|}{|\tilde{\mathbf{B}}_\theta|} \approx \frac{e\cdot\delta n_e|\mathbf{v}_\theta|}{e\cdot\delta n_e|\mathbf{v}_z|} = \frac{|\mathbf{v}_\theta|}{|\mathbf{v}_z|} = \frac{\Omega_{ia}\cdot R}{\nu_{ia}} = \frac{2\pi D}{\lambda_p}. \tag{13}$$

This ratio proved to be of kinematic nature and this follows from a *solid body* rotation of the charged solenoid (Fig. 1): the slow axial current producing weak tangential field $|\tilde{\mathbf{B}}_\theta|$ is due to IAW translational motion while a fast tangential speed $\Omega_{ia}R$ produces the large axial induction ($|\tilde{\mathbf{B}}_z|$).

Apart from the isolated double helix interference pattern having diameter near $D \approx 100$ μm in the proposed loop collider setup (Fig. 2), the more complex experimental situation appears in a speckle produced by RPP [9]. The optical vortices in a RPP speckle have a size of 6–100 μm [7,9–11]. Thus the pump field $\mathbf{E}_p$ distorted by RPP may produce a definite PC component in the Stockes wave $\mathbf{E}_s$ reflected from a plasma jet due to standard SBS-PC mechanism [11]. Recently it was pointed out that optical speckle consists of randomly spaced set of a vortex–antivortex pairs [15,14]. The analogous vortex–antivortex pairs might occur in an underdense plasma as well because of a similarity of SBS mechanisms in both cases [9]. Consequently the rotating charges in a plasma are expected to be a sources of the local counter-directed *dc* magnetic dipoles. These dipoles should be collocated with a plasma vortices having doubled topological charge 2ℓ [13,14]. Such essentially **3D** feature of plasma turbulence may be revealed by numerical investigation in (z, x, y, t) dimension [22] with $\lambda_{ia} \approx \lambda_p/2$ resolution instead of low resolution (z, x, t) numerical experiments in slowly varying envelope approximation [9]. For the sufficiently large values of the local magnetic induction ($|\tilde{\mathbf{B}}| \sim 10^6$ G) the back action of the magnetic field upon plasma currents would be possible. Noteworthy also the related task concerning a collision in a plasma of the two few cycle femtosecond optical vortices with mutually conjugated wavefronts.

5. Conclusion

In summary we have shown that the nonrelativistic plasma vortex flow resonantly initiated by SBS of the two phase-conjugated optical vortices is capable to produce a kilogauss quasi-static magnetic field in a thin slice of the preformed underdense plasma jet [7]. In accordance with our model (e.g. (2), (8), (10), (11)) the particles from a preformed thermal bath having keV temperatures (e.g. $T_i \approx 0.25$ keV, $T_e \approx 0.4$–0.7 keV [7]) are accelerated by rotating maxima of light intensity by virtue of ponderomotive force and acquire the azimuthal speed $v_\theta = \Omega_{ia} R < 0.1 \cdot c$ in addition to axial speed c_{ia} which coincides with the IAW velocity. The azimuthal speed v_θ is about two orders of magnitude bigger compared to an axial one $v_z = c_{ia}$ (13). This provides a corresponding increase of the axial component of magnetic induction $\tilde{\mathbf{B}}_z$ compared to the azimuthal one $\tilde{\mathbf{B}}_\theta$. The axial Tesla-range static magnetic fields proposed here in rotating plasma microsolenoid setup might be interesting from the point view of studies of the vacuum birefringence phenomena where a first results had been obtained quite recently in the PVLAS experiment [34] (noteworthy the different mutual orientation of the laser axis and magnetic induction in our case).

The case of relativistic intensities and femtosecond laser duration $\tau \approx 10^{-14-15}$ s in a geometry (Fig. 2) was not studied yet and this case deserve a particular consideration. Nevertheless it is worth to mention the else interesting feature of the rotating interference pattern described by (2). For the sufficiently large radius R_{sl} the speed of the azimuthal motion v_θ of the optical interference pattern may reach or even exceed the speed of light in a vacuum $\Omega_{ia} R_{sl} \geqslant c$. It is well known that such a superluminal motion of the interference maxima does not violate casuality because formula (2) presumes the overlapping of infinitely long pulses. As is shown previously for the “fast light” phenomena [35] the interference maxima cannot transfer the superluminal signal thus casuality is maintained. The same situation holds for the nonlinear laser amplifiers [36,37] and optical pulses in dispersive medium [38]. In our case when azimuthal speed of rotation v_θ approaches c, the actual relativistic plasma flow will be different from the above formulated nonrelativistic SBS model which presumes the collocation of the optical intensity maxima and plasma current.

Acknowledgement

The partial support of the Russian fund for Basic Research Grant 08-02-01229 is acknowledged.

References

[1] A.F. Alexandrov, L.S. Bogdankevich, A.A. Rukhadze, Principles of Plasma Electrodynamics, Springer-Verlag, Berlin, 1984.
[2] W.L. Kruer, The Physics of Laser Plasma Interactions, Addison–Wesley, New York, 1990.
[3] C.S. Liu, M.N. Rosenbluth, R.B. White, Phys. Fluids 17 (1974) 1211.
[4] P.M. Lushnikov, H.A. Rose, Phys. Rev. Lett. 92 (2004) 255003.
[5] H.A. Baldis, C. Labaune, E. Schifano, N. Renard, A. Michard, Phys. Rev. Lett. 77 (1996) 2597.
[6] R.K. Kirkwood, et al., Phys. Plasmas 4 (1997) 1800.
[7] C. Labaune, H.A. Baldis, V.T. Tikhonchuk, Europhys. Lett. 38 (1997) 31.
[8] A.V. Maximov, I.G. Ourdev, D. Pesme, W. Rozmus, V.T. Tikhonchuk, C.E. Capjack, Phys. Plasmas 8 (2001) 1319.
[9] P. Loiseau, et al., Phys. Rev. Lett. 97 (2006) 205001.
[10] N.G. Basov, I.G. Zubarev, A.B. Mironov, S.I. Mikhailov, A.Y. Okulov, JETP 52 (1980) 847.
[11] B.Y. Zeldovich, N.F. Pilipetsky, V.V. Shkunov, Principles of Phase Conjugation, Springer-Verlag, Berlin, 1985.
[12] J.F. Nye, M.V. Berry, Proc. R. Soc. London, Ser. A 336 (1974) 165.
[13] A.Yu. Okulov, J. Phys. B 41 (2008) 101001.
[14] A.Yu. Okulov, Phys. Rev. A 80 (2009) 163907.
[15] A.Yu. Okulov, JETP Lett. 88 (2008) 631.
[16] R. Marchiano, F. Coulouvrat, L. Ganjehi, J.-L. Thomas, Phys. Rev. E 77 (2008) 016605.
[17] J.W.R. Tabosa, D.V. Petrov, Phys. Rev. Lett. 83 (1999) 4967.
[18] M. Woerdemann, C. Alpmann, C. Denz, Opt. Express 17 (2009) 22791.
[19] V.N. Tsytovich, Phys. Usp. 177 (2007) 428.
[20] M.G. Haines, Phys. Rev. Lett. 87 (2001) 135005.
[21] V.Yu. Bychenkov, V.I. Demin, V.T. Tikhonchuk, JETP 78 (1994) 62.
[22] Z. Najmudin, et al., Phys. Rev. Lett. 87 (2001) 215004.
[23] J. Leach, M.J. Padgett, S.M. Barnett, S. Franke-Arnold, J. Courtial, Phys. Rev. Lett. 88 (2002) 257901.
[24] M. Borghesi, A.J. MacKinnon, A.R. Bell, R. Gaillard, O. Willi, Phys. Rev. Lett. 80 (1998) 112.
[25] M. Borghesi, A.J. Mackinnon, R. Gaillard, O. Willi, A. Pukhov, J. Meyer-ter-Vehn, Phys. Rev. Lett. 81 (1998) 5137.
[26] F.N. Beg, et al., Phys. Rev. Lett. 92 (2004) 095001.
[27] V.Yu. Bychenkov, V.P. Silin, V.T. Tikhonchuk, JETP 71 (1990) 709.
[28] V.P. Krainov, J. Phys. B 36 (2003) 3187;
V.P. Krainov, JETP 96 (2003) 430.
[29] R.N. Sudan, Phys. Rev. Lett. 70 (1993) 3075.
[30] V.S. Belyaev, V.P. Krainov, V.S. Lisitsa, A.P. Matafonov, Phys. Usp. 51 (2008) 428.
[31] L. Allen, M.W. Beijersbergen, R.J.C. Spreeuw, J.P. Woerdman, Phys. Rev. A 45 (1992) 8185.
[32] G.A. Mourou, T. Tajima, S.V. Bulanov, Rev. Mod. Phys. 78 (2006) 309.
[33] E.M. Lifshitz, L.P. Pitaevskii, Physical Kinetic, Landau and Lifshitz Course of Theoretical Physics, Butterworth–Heineman, Oxford, 1982.
[34] M. Marklund, P.K. Shukla, Rev. Mod. Phys. 78 (2006) 591640.
[35] B.M. Bolotovskii, A.V. Serov, Phys. Usp. 48 (9) (2005) 903.
[36] R.V. Ambartsumyan, N.G. Basov, V.S. Letokhov, et al., JETP 23 (1966) 16.
[37] A.Yu. Okulov, A.N. Oraevskii, Sov. J. Quantum Electron. 18 (2) (1988) 233.
[38] R.Y. Chiao, Phys. Rev. A 50 (1993) R34.